Advances in Science and Technology Vol. 58 (2008) pp 237-246
online at http://www.scientific.net

Online available since 2008/Sep/02

Vortex Rings in Bio-inspired and Biological Jet Propulsion

Paul S. Krueger[1, a], Ali A. Moslemi[1,b], J. Tyler Nichols[1,c], Ian K. Bartol[2,d], and William J. Stewart[2,e]

[1]Department of Mechanical Engineering, Southern Methodist University, Dallas, TX, USA

[2]Department of Biological Sciences, Old Dominion University, Norfolk, VA, USA

[a]pkrueger@engr.smu.edu, [b]amoslemi@smu.edu, [c]tyler.nichols@lmco.com, [d]ibartol@odu.edu, [e]wstewart@uci.edu

Keywords: Vortex rings, pulsed jets, propulsion, thrust, propulsive efficiency.

Abstract. Pulsed-jets are commonly used for aquatic propulsion, such as squid and jellyfish locomotion. The sudden ejection of a jet with each pulse engenders the formation of a vortex ring through the roll-up of the jet shear layer. If the pulse is too long, the vortex ring will stop forming and the remainder of the pulse is ejected as a trailing jet. Recent results from mechanical pulsed-jets have demonstrated that vortex rings lead to thrust augmentation through the acceleration of additional ambient fluid. This benefit is most pronounced for short pulses without trailing jets. Simulating vehicle motion by introducing background co-flow surrounding the jet has shown that vortex ring formation can be interrupted, but only if the co-flow is sufficiently fast. Recent in situ measurements on squid have captured vortical flows similar to those observed in the laboratory, suggesting thrust augmentation may play a role in their swimming performance. Likewise, recent measurements with a mechanical self-propelled pulsed-jet vehicle ("robosquid") have shown a cruise-speed advantage obtained by pulsing.

Introduction

Vortex rings are surprisingly common flow phenomena. They may be generated by surface tension effects, buoyant plumes, flow separation from the unsteady motion of a solid boundary, or momentum driven jets [1]. In the case of the latter, vortex rings are generated by the transient ejection of a jet from a tube or orifice, which leads to the roll-up of the jet shear layer into a toroidal ring that propagates downstream under its own self-induced velocity in accordance with Helmholtz laws of vortex motion. In effect, any unsteady jet flow can lead to vortex rings or flow structures that resemble vortex rings. This is apparent in a wide range of natural and man-made flows ranging from synthetic jet actuators [2] to volcanic eruptions.

Unsteady jets in the form of a series of jet pulses are a common method of aquatic propulsion utilized by squid and jellyfish among others. Recent investigations of squid and jellyfish locomotion have demonstrated vortex ring formation during pulsed jet propulsion for several squids and jellyfishes. Parallel studies of mechanically generated pulsed jets have revealed key advantages of pulsed jet propulsion and their relationship to vortex ring formation. This paper discusses key features of vortex ring formation by pulsed jets and their relationship to propulsion, recent results of studies of biological and biomimetic pulsed-jet propulsion, and ongoing work by the authors investigating pulsed-jet performance in different scenarios.

Background on Mechanical and Biological Pulsed Jets

Vortex Ring Generating Mechanisms. A simple method for generating a transient jet (jet pulse) is to eject a finite amount of fluid from a nozzle in a time t_p by translating a piston through a distance L as shown in Fig. 1(a). This device is known as a piston-cylinder mechanism and L/D is the stroke-ratio of the pulse. The functional form of the jet velocity variation, $U_J(t)$, is known as the velocity program. When the external fluid is initially quiescent, the jet is called a starting jet.

Ejecting pulses periodically while ensuring a period of no flow between pulses provides a vortex ring with each pulse. This situation is commonly termed a fully-pulsed jet or fully-modulated jet [3, 4]. Practically speaking, fully-pulsed jets require a separate inlet to generate continuous pulsing, but for simplicity, this is not shown in Fig. 1.

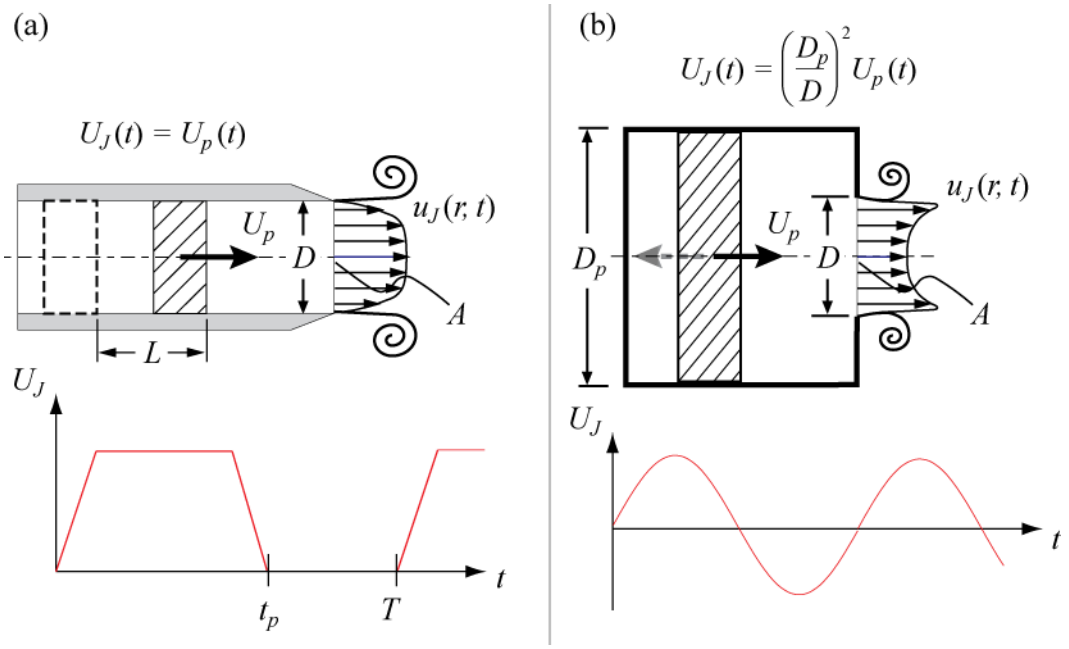

Figure 1. Mechanical Vortex Ring Generation: (a) Pulsed-jet generated by a piston-cylinder mechanism; (b) Synthetic jet generated by an oscillating piston (or membrane) in a cavity.

A related method for generating jet pulses is a synthetic jet, which is illustrated in Fig. 1(b). In this case the jet driver oscillates in place so that the average mass flux of the jet is zero. Outside the Stokes limit, such devices exhibit a net momentum flux and positive thrust is generated [5, 6]. Synthetic jets can generate continuous thrust indefinitely using a vanishingly small plenum, but the boundary motion generating the jet is time-reversible, making them ineffective in the Stokes limit.

There are numerous biological analogs to the mechanical methods for generating pulsed jets. Two canonical cases are squid and jellyfish. A schematic of typical squid locomotion is illustrated in Fig. 2(a). The squid propulsion cycle begins by expanding the mantle, a large muscular organ enclosing an internal cavity. Expanding the mantle draws fluid into the mantle cavity via ducts surrounding the head. Circular muscles in the mantle then contract, which increases the fluid pressure in the mantle, closes the inlet valves, and forces the fluid out of the funnel (nozzle) [7]. The funnel may be directed in a hemisphere below the body of the squid so that the squid may be propelled forward or backward, hover in place, or turn in place. Squid also exhibit active control over the funnel diameter during jet ejection [7, 8, 9]. Jellyfish, in contrast, have only one orifice used for both fluid ingestion and ejection, as shown in Fig. 2(b). For propulsion, jellyfish expand the bell, drawing fluid into the sub-umbrellar cavity through the bell margin. Contracting the umbrella forces fluid out the same orifice and propels the jellyfish in the opposite direction [10]. (It should be noted that some species of jellyfish exhibit non-uniform bell contraction, leading to a combination of jet-type and rowing-type propulsion [11].)

Recent observations using both dye visualization and digital particle image velocimetry (DPIV) have demonstrated vortex ring formation by jet pulses from both squid and jellyfish propulsion [12, 13, 14]. Although both squid and jellyfish have features not present in the mechanical analogs (most notably, variable exit diameters), it is apparent that squid propulsion is functionally most similar to fully-pulsed jets while jellyfish are most similar to synthetic jets. In particular, both jellyfish and synthetic jets use the same orifice for fluid ingestion and ejection, and both use time-reversible boundary motion. In the interest of brevity, the remainder of this paper will focus on starting jets and fully-pulsed jets.

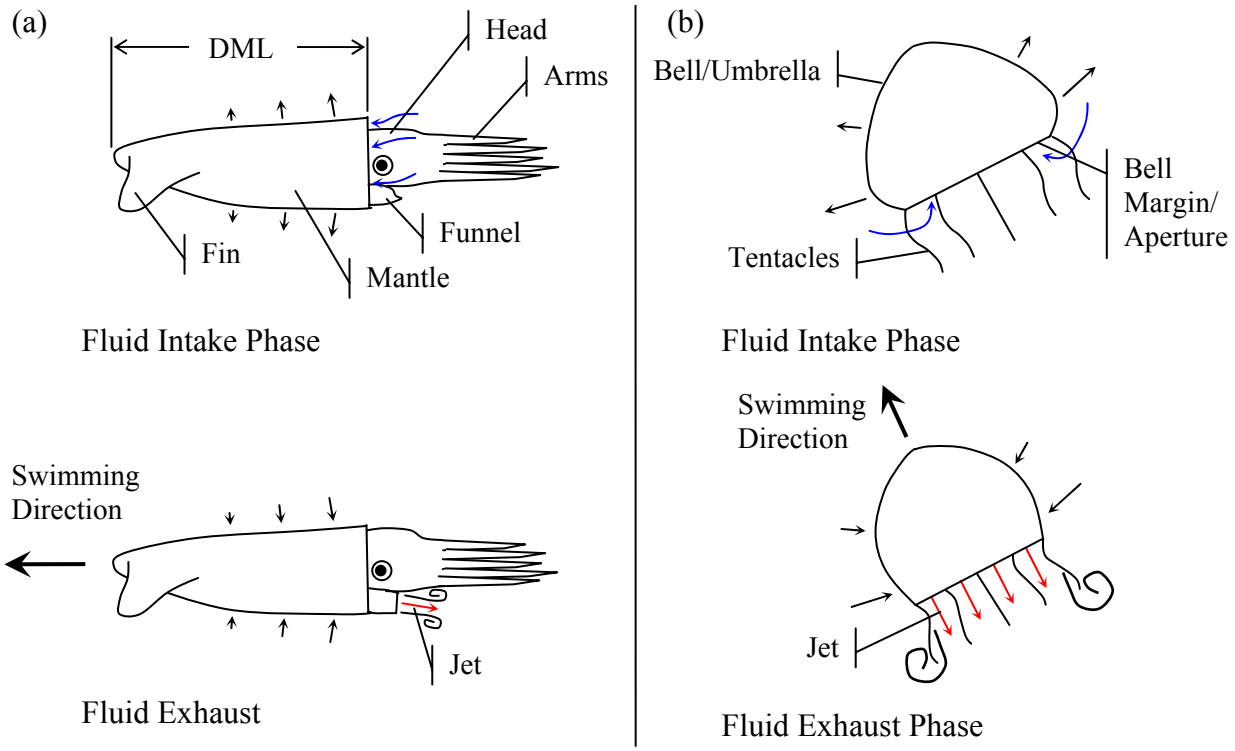

Figure 2. Biological Jetters: (a) General anatomy of a squid and description of the jet actuation mechanism. The squid is shown swimming in the tail-first orientation. DML = Dorsal Mantle Length. (b) General anatomy of a jellyfish and the jet generation sequence.

Vortex Rings and Thrust. Key advantages of vortex ring formation for propulsive applications are discussed in this section. The majority of the results are derived from investigations utilizing mechanical vortex ring generators. The relationship with biological or biomimetic propulsion will be discussed in subsequent sections.

For propulsive applications, a key parameter related to vortex rings is the total impulse, **I**, required to generate the flow. For an isolated vortex ring, **I** is the hydrodynamic impulse of the vortex ring, which has magnitude I and is directed in the direction of motion of the vortex ring. For a steadily translating vortex ring, it can be shown that

$$I = \left(m_{EJ} + m_E + m_A\right)W \tag{1}$$

where m_{EJ} is the mass of fluid ejected from the nozzle, m_E is the mass of the ambient fluid entrained into the vortex ring bubble, and m_A is the added mass associated with the fluid motion surrounding the vortex ring bubble [15]. The ejected and entrained mass represent the total fluid mass contained within the closed streamline surrounding the vortex ring in a frame of reference traveling with the vortex ring. Eq. 1 indicates that the impulse of the vortex ring is due to more than just the momentum of the ejected fluid.

The vortex ring impulse is imparted by the generating jet. The jet impulse can be expressed as

$$I = \underbrace{\rho \int_0^{t_p} \int_A u_J^2(r,t)\,dA\,dt}_{I_U} + \underbrace{\int_0^{\infty} \int_A \left[p(r,t) - p_\infty\right] dA\,dt}_{I_p} \tag{2}$$

where ρ is the fluid density, u_J is the jet velocity at the nozzle exit plane, p is pressure, A is the cross-sectional area of the jet at the nozzle exit plane, I_U is the impulse from the jet momentum, and I_p is impulse from over-pressure at the jet exit plane. Due to the transient nature of the jets used to generate vortex rings, I_p can be a significant fraction of I, especially in the case of starting jets. As a consequence, the impulse provided per pulse can be much larger than that due to the jet momentum alone and steady-jet approximations underestimate I [15].

Combining Eqs. 1 and 2 it is apparent that the extra impulse supplied by I_p is related to the additional mass accelerated with the vortex ring (m_{EN} and m_A) during formation. This observation was inferred from bulk measurements if I and I_U by Krueger and Gharib [15]. In a recent numerical investigation of vortex ring formation, Lagrangian Coherent Structures (LCS) were used to identify and track the different fluid regions throughout vortex ring formation to precisely quantify the breakdown of impulse between m_{EJ}, m_E, and m_A [16]. A typical result is shown in Fig. 3. As illustrated in Fig. 3, added mass accounts for the largest fraction of I once the formation process is completed ($t/t_p > 2$). Similar results hold for different L/D and jet velocity programs, but show larger fractions of impulse associated with added mass for shorter L/D and velocity programs that decelerate more slowly.

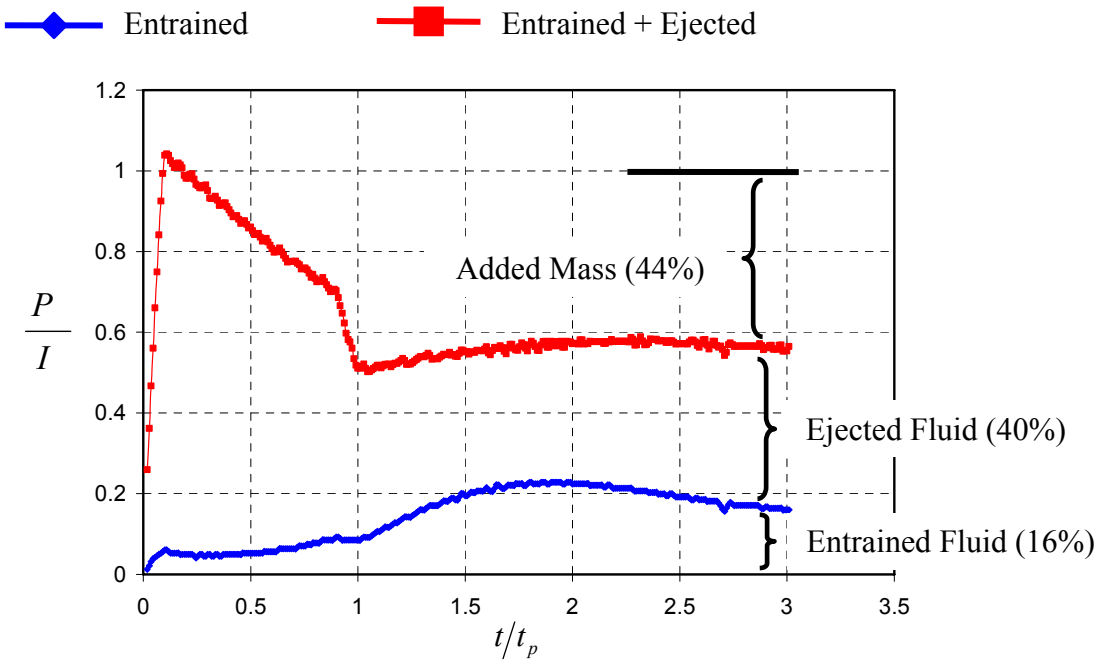

Figure 3. Time Evolution of the Momentum (P) of the Entrained and Ejected Fluid. I is the impulse of the vortex ring when it has reached steady state. This data is for $L/D = 2$ with a trapezoidal velocity program and a jet Reynolds number of 1000.

From these observations, it is clear that the extra impulse supplied by starting jets, over and above that of the jet momentum, is primarily related to the acceleration of additional ambient fluid during vortex ring formation as the forming ring pushes ambient fluid out of the way (added mass effect). When periodic pulses are utilized to continuously generate thrust via a fully-pulsed jet, the additional impulse supplied by vortex ring formation leads to thrust augmentation [3, 17]. That is, when compared to a steady jet of either identical mass flux only or identical mass and momentum flux, the thrust produced by a pulsed jet is larger. For pulsed and steady jets of identical mass flux, the pulsed jet can have more than twice the thrust of the steady jet [3]. Of course, anything that disrupts the contribution of added mass to vortex ring impulse tends to disrupt augmentation. In particular, augmentation based on comparison with a steady jet of identical mass and momentum

flux tends to decrease as pulses become closer together, indicating that added mass and its associated over-pressure effects are reduced as the ambient fluid can no longer be considered quiescent.

Generally the effect of vortex ring formation on thrust augmentation is enhanced the larger the vortex ring (i.e., larger vortex rings implies greater thrust augmentation). Thus, it is tempting to utilize long pulses in order to maximize the size/strength of the resulting vortex rings. Very long duration pulses, however, approach steady jet behavior rather than generating an enormous vortex ring. Gharib et al. [18], showed that for L/D beyond a critical value, called the formation number (F), vortex rings stop forming and the remainder of the fluid is ejected as a quasi-steady "trailing jet" following the leading vortex ring. Although F can take on a range of values depending on the velocity program [19, 20], the velocity profile at the jet exit plane [20], and the time-variation of the jet diameter [19, 21], $F \approx 4$ for a wide range of conditions.

If the trailing jet has quasi-steady behavior, one can expect that the I_p associated with the unsteady vortex ring formation is less significant for $L/D > F$. This observation was borne out in the experiments of Krueger and Gharib [15], which showed that the average thrust during a pulse is maximized for pulses with L/D near the formation number because longer jets did not contribute as much impulse per unit of ejected fluid during the ejection of the trailing jet. Measurements and cutouts of the associated flow states are given in Fig. 4. Consequently, pulsing with L/D near the formation number is expected to provide optimal thrust augmentation. The pulsed-jet experiments of Krueger and Gharib [3] corroborated this, at least in the limit of low pulsing frequency where interaction between pulses was minimal.

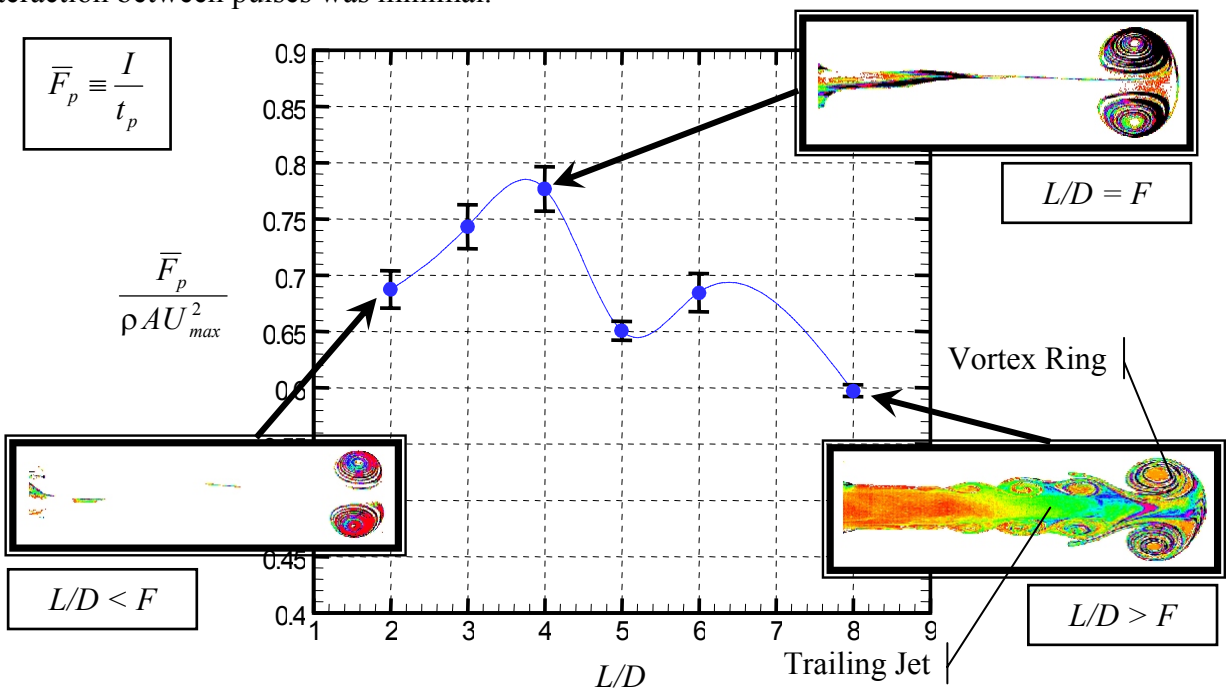

Figure 4. Maximization of Average Thrust During a Pulse for Jet Pulses Near the Formation Number (F). The data is taken from Krueger and Gharib [15] and the starting jet images are from Gharib et al. [18].

All of the results considered thus far are for stationary/tethered jets. For propulsive applications, however, the jet generating mechanism must be allowed to move, which introduces a background co-flow surrounding the jet. This co-flow can influence vortex ring development associated with jet pulses. Krueger et al. [22, 23] showed that the circulation (and presumably the impulse) of the leading vortex ring is reduced in the presence of simultaneously initiated co-flow, but otherwise the development of the leading vortex ring is unaltered provided the ratio of peak co-flow velocity to peak jet velocity, R_v, is not too large. If R_v is greater than a critical value

(approximately 0.6 in the experiments of Krueger et al. [23]) the development of the leading vortex ring is pre-empted near jet initiation, which would likely eliminate any propulsive benefit associated with a leading vortex ring. Jiang and Grosenbaugh [24] found results similar to Krueger et al. [22, 23] at low velocity ratios using a starting jet ejected into a co-flow initiated at $t \to \infty$ so that a recirculating wake was present at the nozzle exit when the jet was initiated. At higher velocity ratios, the wake was strong enough to disrupt the formation of a leading vortex. One might expect that the results of Krueger et al. [22, 23] are most relevant for vehicle accelerating from rest and the study of Jiang and Grosenbaugh [24] is analogous to steady propulsion. The period between pulses, however, is typically short and squid close their funnel between pulses (preventing the formation of a wake within the funnel) so that steady propulsion may actually be best represented by the results of Krueger et al. [22, 23]. Regardless of which model is most appropriate, it is clear that vehicle velocities approaching the jet velocity can severely disrupt vortex ring formation, likely quelling any propulsive benefits associated with jet pulsation.

Vortex Rings and Propulsive Efficiency. Following Lighthill [25] and Krueger [26], propulsive efficiency of pulsed jets is evaluated using

$$\eta_P = \overline{\dot{W}_u} \Big/ \left(\overline{\dot{W}_u} + \overline{\dot{E}_{ex}} \right) \tag{3}$$

where $\dot{W}_u$ is the rate of useful work done by propulsion, $\dot{E}_{ex}$ is the rate at which excess kinetic energy is shed into the wake, and the over bar denotes the time average. The rate of useful work done by propulsion is $\dot{W}_u \equiv F_T U_v$. Following Lighthill [25] we approximate $\overline{\dot{W}_u} \approx \overline{F}_T U_v$ where $\overline{F}_T = I/T$ is the time-averaged thrust, U_v is the (time-averaged) vehicle velocity, and T is the pulse period (see Fig. 1).

To understand the general behavior of η_P for pulsed jets, we consider a hypothetical case where $U_J = U_0$ is constant during jet ejection and zero otherwise. Then, ignoring non-uniformities in the jet profile, $I_U \approx \Delta m \left(U_J - U_v \right)$ where Δm is the mass of fluid ejected during the jet pulse. Likewise, $\overline{\dot{E}_{ex}} = \overline{\dot{m}} \left(U_{eff} - U_v \right)^2 / 2$ where $\overline{\dot{m}} = \Delta m / T$. By conservation of energy, the effective velocity U_{eff} is determined from $\Delta m U_{eff}^2 / 2 = E_U + E_p \equiv E$ where E_U is the kinetic energy exhausted into the wake during t_p (in the frame of reference moving at U_v) and E_p is the work done by over-pressure. Combining these results with Eq. 3 and simplifying gives

$$\eta_P = \frac{2R_v}{2R_v + \left(\dfrac{1 - I_p/I}{1 - R_v} \right) \left(\dfrac{1}{\sqrt{1 - E_p/E}} - R_v \right)^2} \tag{4}$$

where $R_v = U_v / U_0$ is the vehicle-to-jet velocity ratio ($0 \le R_v \le 1$ for propulsive applications).

Eq. 4 indicates an interesting competition between I_p and E_p. If I_p/I is large (close to 1), then η_P is driven toward 1 for all R_v, but an E_p/E close to 1 can counter this effect. Typical measurements for these quantities in stationary jets give I_p/I around twice that of E_p/E so that the impulse term out weighs the pressure-work term. Thus, the additional impulse provided by vortex ring formation also tends to be beneficial for propulsive efficiency as well. Note also that for steady jet propulsion, $I_p/I = E_p/E = 0$ and Eq. 4 reduces to the result for Froude efficiency.

Eq. 4, however, is approximate in the sense that all unsteady effects are lumped into I_p/I and E_p/E while explicit temporal and spatial variations in u_J are ignored.

Vortex Rings and Thrust Augmentation in Pulsed-Jet Propulsion

The preceding discussion illuminates the key role played by vortex ring formation in propulsion using pulsed jets, but also highlights the general lack of data for pulsed jets in realistic, self-propelled settings. Detailed data for such cases is only recently becoming available. Some preliminary results for two investigations are discussed below.

Robosquid. A mechanical, self-propelled, pulsed-jet vehicle (Robosquid) has recently been developed at SMU for purposes of studying the propulsive efficiency of pulsed-jet propulsion with particular emphasis on the scaling of η_P as vehicle Reynolds number is decreased. A schematic of the Robosquid is shown in Fig. 5. Robosquid is propelled by a linear actuator that oscillates a piston back and forth. During the power stroke, fluid is drawn in through slots just behind the actuator and simultaneously ejected rearward from the nozzle. During the recovery stroke, the piston is pulled back to its original position. Check valves downstream of the intake slots prevent fluid ejection from escaping through the inlet and check valves embedded in the piston allow fluid behind the piston to be displaced to the other side as the piston moves backward. A small amount of fluid (~5% of that ejected) is drawn back into the nozzle during the recover stroke due to the reduced fluid volume behind the piston caused by the presence of the actuator shaft, but this effect is small and the flow well-approximates a fully-pulsed jet.

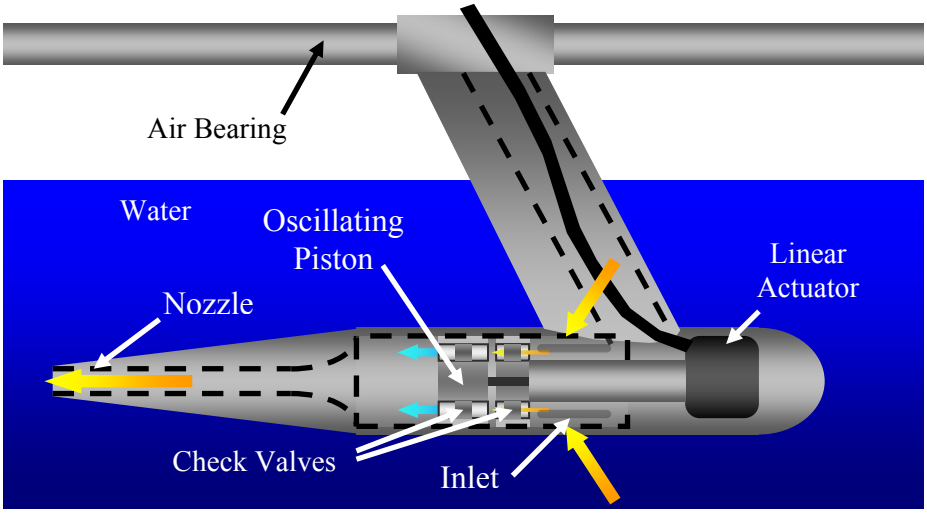

Figure 5. Schematic of Robosquid.

Initial experiments with Robosquid have tested its speed in water as a function of various pulsing parameters. Of key interest here is how well this compares with propulsion by an equivalent steady jet. One such comparison is the vehicle speed for pulsed-jet propulsion vs. steady jet propulsion. This comparison is shown in Fig. 6 for a pulsed jet using a 50% duty cycle and isosceles triangular jet velocity programs. The equivalent steady jet speed was determined based on the thrust from a steady jet with the same time-averaged mass flux and CFD estimates of the drag coefficient for Robosquid during steady jet propulsion. The increase in $U_{v,pulsed}/U_{v,steady}$ with L/D is because the maximum jet velocity increased with L/D for this particular test. Although the results are limited, they show a clear speed advantage for pulsed jet propulsion, which is indicative of the thrust augmentation expected from the results of Krueger and Gharib [3]. Future experiments will consider $L/D < 4$ and the effects of pulse duty cycle using DPIV to measure thrust augmentation directly and also determine propulsive efficiency.

In-Situ Measurements of Swimming Squid. In a recent study, Bartol et al. [12] used DPIV to measure the flow field produced by squid jet propulsion in steadily swimming juvenile and adult brief squid *Lolliguncula brevis*. Swimming was observed in a 15 cm x 15 cm test section water tunnel using a movable laser sheet and camera traverse so that DPIV measurements bisecting the jet could be obtained. A total of 50 jet sequences from individuals ranging in size from 2.0 cm to 8.5 cm dorsal mantle length (DML) and swimming over a range of speeds from 2.4 to 18.6 cm s^{-1} (0.8 – 3.2 DML s^{-1}) were considered. Over these swimming sequences, both short jet pulses and long pulses were observed as shown in Fig. 7. The short pulses produced isolated vortex rings (Fig. 7(a)) and the resulting flow was called *Jet Mode I*. Longer pulses lead to formation of a leading vortex ring pinched off from its generating jet (Fig. 7(b)), which was called *Jet Mode II*. While both jet modes were observed across all swimming speeds, *Jet Mode I* was preferred for slower swimming speeds.

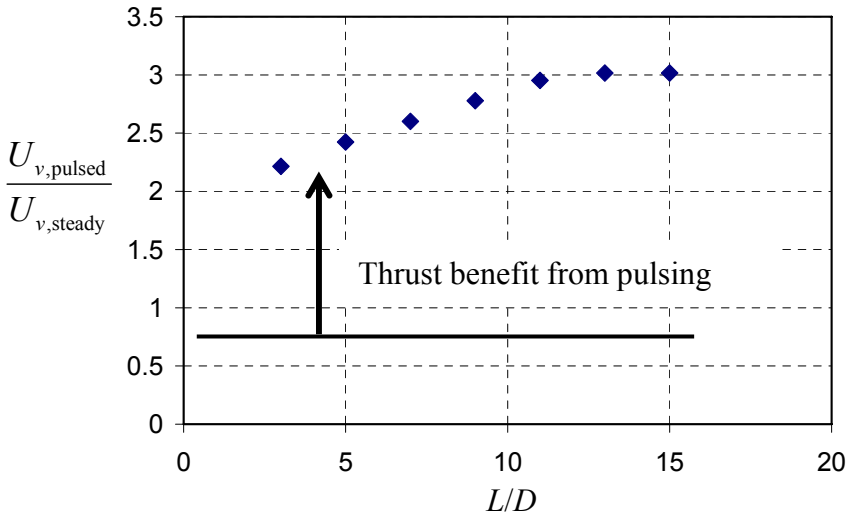

Figure 6. Representative Data for the Speed of Robosquid. The pulsed jet for these results used an isosceles triangular velocity program with a 50% duty cycle.

The remarkable similarity between *Jet Mode I* and mechanically generated vortex rings and between *Jet Mode II* and mechanically generated starting jets with $L/D > F$ is undeniable (cf. Fig. 7 and Fig. 4). Although the jet slug length to funnel diameter ratio was not measured directly for these flows, the ratio of the length of the jet (based on the extent of the velocity field) to the maximum funnel diameter ranged from 3.87 – 7.84 for *Jet Mode I* and 6.97 – 20 for *Jet Mode II*. These values probably underestimate the actual L/D because the extent of the velocity field tends to be smaller than L for $L/D > 1$. Thus, the L/D for *Jet Mode I* extends beyond the usual value of 4 for the formation number. This is likely due to the fact that a) co-flow has not been accounted for (background co-flow tends to delay pinch off to larger ejected slug lengths [22, 23]) and b) variation of the jet diameter and/or jet velocity can delay pinch off to larger formation numbers [19, 21]. The similarity of *Jet Mode II* with pinch off observed in mechanically generated starting jets is also noteworthy because the jet flow is inclined relative to the background flow. Pinch off in this configuration has not been studied in detail for mechanically generated jets.

Propulsive efficiency of squid jet locomotion were calculated using Eq. 3 and measurements of $\overline{F}_T$ and $\overline{\dot{E}}_{ex}$ from the hydrodynamic impulse and kinetic energy of the jet, respectively, assuming axisymmetry of the jet flow field. (Only the component of impulse in the direction of locomotion was used in computing thrust.) The mean η_P for all cases measured was 77.8 $\pm$ 11.6% (mean $\pm$ S.D.). For *Jet Mode I*, $\eta_{P,I}$ = 80.7 $\pm$ 10.2%, which was significantly higher than the efficiency of *Jet Mode II*, namely, $\eta_{P,II}$ = 71.3 $\pm$ 13.3%. From Eq. 4, a higher efficiency for *Jet Mode I* is expected because *Jet Mode II* is approaching steady jet flow for which $I_p/I = 0$, whereas I_p/I is

expected to be substantial for isolated vortex rings as occur in *Jet Mode I*. Apparently increases in I_p/I outweighed increases in E_p/E for *Jet Mode I*.

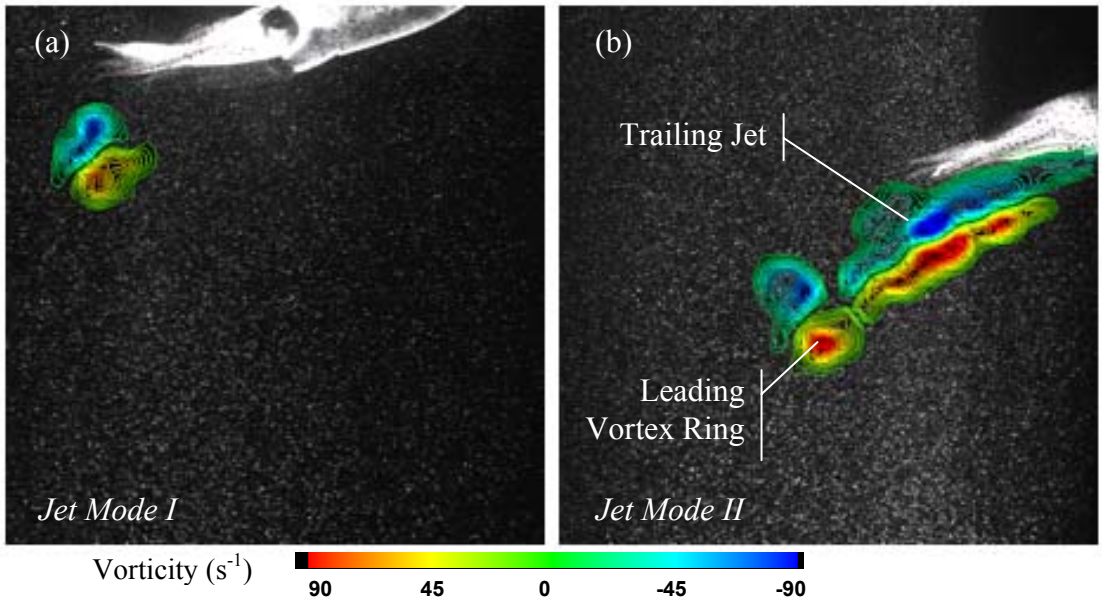

Figure 7. DPIV Measurements of a Swimming *Lolliguncula brevis*: (a) a 4.2 cm DML *L. brevis* swimming at 6 cm s^{-1} (1.43 DML s^{-1}); (b) a 6.2 cm DML *L. brevis* swimming at 10 cm s^{-1} (1.61 DML s^{-1}).

The efficiency of *Jet Mode I* could also be enhanced by the fact that fin motion contributes more to propulsion at slow speeds (where this mode is more prevalent), giving a larger U_v than expected from jet thrust alone. This is unlikely, however, given that measurements of *Doryteuthis pealeii* hatchlings in the same study exhibited jet flows similar to *Jet Mode I* at even higher jet efficiencies with no significant input from the fins.

Data from this study represent, perhaps, the clearest link between the advantages of pulsed jets with short pulses (isolated vortex rings) over long pulses (vortex rings with trailing jets) or even steady jets for achieving high η_P. It should be noted, however, that not all squid species exhibit the jet modes reported here. Juvenile and adult *D. pealleii*, for instance, produce long pulses with no dominant vortex ring structure [27]. The reason for this difference between species is unclear.

Conclusions and Outlook

Investigations of mechanical pulsed jets demonstrate thrust augmentation via the acceleration of ambient fluid associated with vortex ring formation, but the benefit diminishes for long duration jets where the forming ring pinches off from the generating jet to give a leading vortex ring followed by a trailing jet. Ongoing investigations of a self-propelled pulsed-jet vehicle (Robosquid) illustrate a similar thrust benefit in an untethered setting. The thrust benefit afforded by vortex ring formation requires additional energy as well, but the energy requirement appears to be low compared to the impulse benefit, as swimming squid demonstrate higher propulsive efficiencies for short jet pulses (isolated vortex rings) than long pulses comprised of a vortex ring and trailing jet.

It is interesting to consider whether the propulsive gains achieved by pulsing carry over to small scale propulsion systems. Initial work with *D. pealleii* hatchlings (~2 mm DML) suggests that it does, as comparable or greater propulsive efficiencies have been observed [12]. Future work with Robosquid seeks to quantify the scaling of pulsed jet performance as Reynolds number is decreased and quantify the optimal pulsing conditions for low Reynolds number micro-propulsion applications.

Acknowledgements

The support of the National Science Foundation under grants IOS-0446229 and CTS-0347958 is gratefully acknowledged.

References

[1] K. Shariff, and A. Leonard: Vortex rings. Annu. Rev. Fluid Mech. Vol. 24 (1992) p. 235.

[2] A. Glezer and M. Amitay: Annu. Rev. Fluid Mech. Vol. 34 (2002) p. 503.

[3] P. S. Krueger and M. Gharib: AIAA J. Vol. 43 (2005) p. 792

[4] H. Johari, M. Pacheco-Tougas, and J. C. Hermanson: AIAA J. Vol. 37 (1999) p. 842.

[5] M. O. Muller, L. P. Bernal, R. P. Moran, P. D. Washabaugh, B. A. Parviz, T.-K. A. Chou, C. Zhang, and K. Najafi: AIAA-2000-2404 (2000), AIAA Fluid Dynamics Conference, Denver, CO.

[6] M. Krieg, A. Pitty, M. Salehi, and K. Mohseni: Proc. MTS/IEEE, OCEANS, 2005, Vol. 3 (2005) p. 2342.

[7] E. J. Anderson and M. E. DeMont: J. Exp. Biol. Vol. 203 (2000) p. 2851.

[8] R. K. O'Dor: J. Exp. Biol. Vol. 137 (1988) p. 421.

[9] I. K. Bartol, M. R. Patterson, and R. Mann: J. Exp. Biol. Vol. 204 (2001) p. 3655.

[10] R. M. Anderson: *Principles of Animal Locomotion* (Princeton University Press, Princeton 2003).

[11] S. P. Colin, and J. H. Costello: J. Exp. Biol. Vol. 205 (2002) p. 427.

[12] I. K. Bartol, P. S. Krueger, J. T. Thompson, and W. J. Stewart: Int. Comp. Biol. (in review).

[13] J. O. Dabiri, S. P. Colin, and J. H. Costello: J. Exp. Biol. Vol. 209 (2006) p. 2025.

[14] J. O. Dabiri, S. P. Colin, and J. H. Costello: J. Exp. Biol. Vol. 210 (2007) p. 1868.

[15] P. S. Krueger and M. Gharib: Phys. Fluids Vol. 15 (2003) p. 1271.

[16] A. B. Olcay and P. S. Krueger: Phys. Fluids (in review).

[17] I. M. Choutapalli: *An Experimental Study of a Pulsed Jet Ejector* (Ph.D. Dissertation, Florida State University, Tallahassee, FL, 2006).

[18] M. Gharib, E. Rambod, and K. Shariff: J. Fluid Mech. Vol. 360 (1998) p. 121.

[19] K. Mohseni, H. Ran, and T. Colonius: J. Fluid Mech. Vol. 430 (2001) p. 267.

[20] M. Rosenfeld, E. Rambod, K. Shariff: J. Fluid Mech. Vol. 376 (1998) p. 297.

[21] J. O. Dabiri and M. Gharib: J. Fluid Mech. Vol. 538 (2005) p. 111.

[22] P. S. Krueger, J. O. Dabiri, and M. Gharib: Phys. Fluids Vol. 15 (2003) p. L49.

[23] P. S. Krueger, J. O. Dabiri, and M. Gharib: J. Fluid Mech. Vol. 556 (2006) p. 147.

[24] H. Jiang and M. A. Grosenbaugh: Theor. Comput. Fluid Dyn. Vol. 20 (2006) p. 103.

[25] M. J. Lighthill: J. Fluid Mech. Vol. 9 (1960) p. 305.

[26] P. S. Krueger: Bioinsp. Biomim. Vol. 1 (2006) p. S49.

[27] E. J. Anderson and M. A. Grosenbaugh: J. Exp. Biol. Vol. 208 (2005) p. 1125